Three-dimensional spatial distribution of scatterers in Galeras volcano, Colombia

E. Carcolé,[1] A. Ugalde,[1] and C. A. Vargas[2]

Received 12 January 2006; revised 16 March 2006; accepted 29 March 2006; published 27 April 2006.

[1] A three-dimensional spatial distribution of relative scattering coefficients is estimated for the Galeras volcano, Colombia, by an inversion of the coda wave envelopes from 1564 high quality seismic recordings at 31 stations of the Galeras seismograph network. The inversion reveals a highly non-uniform distribution of relative scattering coefficients in the region for the two analyzed frequency bands (4-8 and 8-12 Hz). Strong scatterers show frequency dependence, which is interpreted in terms of the scale of the heterogeneities producing scattering. Two zones of strong scattering are detected: the shallower one is located at a depth from 4 km to 8 km under the summit whereas the deeper one is imaged at a depth of ~37 km from the Earth's surface. Both zones may be associated with the magmatic plumbing system beneath Galeras volcano. The second strong scattering zone may be related to a deeper magma reservoir that feeds the system. **Citation:** Carcolé, E., A. Ugalde, and C. A. Vargas (2006), Three-dimensional spatial distribution of scatterers in Galeras volcano, Colombia, *Geophys. Res. Lett.*, *33*, L08307, doi:10.1029/2006GL025751.

1. Introduction

[2] Galeras volcano (1.23°N, 77.36°W; summit elevation 4,276 m) is a 4,500 years old active cone of a more than 1 Ma old volcanic complex which is located in the Central Cordillera of the southwestern Colombian Andes (Figure 1). It is historically the most active volcano in Colombia and it has been re-activated frequently in historic times [*Banks et al.*, 1997]. It is located only 9 km west of the city of San Juan de Pasto which has a population of more than 300,000 and another 100,000 people live around the volcano. Although it has a short-term history of relatively small-to-moderate scale eruptions, the volcanic complex has produced major and hazardous eruptions [*Calvache et al.*, 1997] thus constituting a potential risk to the human settlements in this region. Galeras was designated a Decade Volcano in 1991, which identified it as a target for intensive and interdisciplinary study during the United Nations' International Decade for Natural Disaster Reduction.

[3] The re-activation of Galeras volcano was recognized in 1988 after forty years of repose [*Williams et al.*, 1990] and the eruptive period lasted until 1995. Since then, the volcano has been in a relatively calm stage with some ash and gas emission episodes and low-level eruptive activity. A crater located to the east of the main one was re-activated in 2002 after more than 10 years of inactivity. A new eruptive episode consisting of three explosive events began in 2004 and it continues active at the time of this writing.

[4] Seismicity in the region since 1988 has been characterized by long period events, volcano-tectonic earthquakes and tremor episodes. A type of unusual shallow-source, low frequency seismic signals called "tornillos" which are related to magmatic activity have also been recorded during different stages of volcanic activity at Galeras [*Gómez and Torres*, 1997]. The level of seismic activity has fluctuated, alternating periods of low-level seismicity with episodes of increased seismic activity in terms of the number and/or magnitude of the events. Some shallow (up to 8 km) volcano-tectonic earthquakes have reached local magnitudes up to 4.7.

[5] With the aim of enlarging the knowledge of the internal structure of the volcano as well as to serve for its seismic hazard assessment, the present study is a different complementary contribution to the interdisciplinary research (geological, geophysical and geochemical) being conducted in the region since the re-activation of Galeras volcano. We will focus on the imaging of small-scale heterogeneities by estimating the three-dimensional spatial distribution of relative scattering coefficients from shallow earthquakes that occurred under the volcano region.

2. Data and Method

[6] Data used in this study is a selection of 1564 high quality records of the S-wave coda from shallow earthquakes (depths less than 10 km from the Earth's surface) with local magnitudes less than 2.0 which occurred in the region from 1989 to 2002. The 31 short-period (T_0 = 1 s), vertical component recording stations used were deployed at different stages of the Galeras seismic network operation and they were located at distances less than 10 km from the active crater (Figure 1).

[7] In order to estimate the inhomogeneous spatial distribution of relative scattering coefficients in the crust we followed the method proposed by *Nishigami* [1991] by using an inversion method of coda waveforms from local earthquakes. This method assumes that the fluctuation of the decay curve of the observed coda envelope is caused by a non-uniform distribution of scatterers. The decay curve is then compared with a reference curve, which is estimated by assuming single isotropic scattering and spherical radiation from the source. This method with some adaptations has proved to be an effective approach to investigate the real heterogeneous structure in the crust of several regions in the world [*Nishigami*, 1991, 1997, 2000; *Chen and Long*, 2000; *Asano and Hasegawa*, 2004; *Ugalde et al.*, 2006].

[1] Observatori de l'Ebre, CSIC—Universitat Ramon Llull, Roquetes, Spain.
[2] Departamento de Geociencias, Universidad Nacional de Colombia, Bogotá, Colombia.

0094-8276/06/2006GL025751$05.00

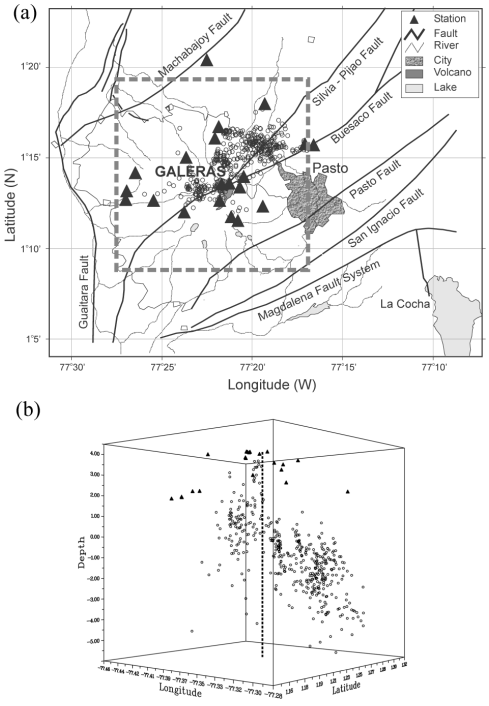

Figure 1. Map of the Galeras volcanic complex region showing the location of the epicenters and seismic stations used: (a) horizontal projection at the surface where the study area is indicated by a dotted square; and (b) a 3-D representation of the stations and hypocenters location.

[8] According to *Nishigami* [1991] the observational system of equations relating the spatial distribution of relative scattering strength to the observed coda energy residuals under the assumption of single isotropic scattering and spherical radiation of a seismic source can be written as:

$$\begin{aligned} w_{11}\alpha_1 + \cdots + w_{i1}\alpha_i + \cdots + w_{N1}\alpha_N &= e_1 \\ &\vdots \\ w_{1j}\alpha_1 + \cdots + w_{ij}\alpha_i + \cdots + w_{Nj}\alpha_N &= e_j \\ &\vdots \\ w_{1M}\alpha_1 + \cdots + w_{iM}\alpha_i + \cdots + w_{NM}\alpha_N &= e_M \end{aligned} \tag{1}$$

[9] This system of equations is obtained by dividing the coda of each seismogram into several small time windows, thus having one equation based on (1) for each time window. Also for each time window, the scatterers contributing to the energy density are contained in a spheroidal shell. Therefore, M is the total number of equations (number of seismograms multiplied by the number of coda time windows considered), and N is the total number of scatterers (number of small blocks into which the study region is divided). The right side of equation (1) is called coda wave energy residual (e_j) which measures the ratio of the observed energy density in this part of the coda to the average energy density of the medium [*Sato*, 1977], and the unknowns $\alpha_i \geq 0$ are the spatial perturbations of the average scattering coefficient of the medium due to an individual scatterer. The weights w_{ij} are defined as:

$$w_{ij} = \frac{1}{\sum_i \frac{1}{(r_{1,i}r_{2,i})^2}} \frac{1}{(r_{1,i}r_{2,i})^2} \tag{2}$$

where $r_{1,i}$ and $r_{2,i}$ are the distances between the hypocenter and the scatterer i and the scatterer i and the station, respectively.

[10] To solve systems of equations as large as (1) there are some powerful iterative and non-iterative methods [e.g., *Kak and Slaney*, 1988] that were first successfully used in tomographic imaging for medical applications and that have been extended to other scientific fields. A very convenient non-iterative method is the Filtered Back-Projection (FBP) algorithm which has proved to be about 100 times faster than the Algebraic Reconstruction Technique (ART) or Simultaneous Iterative Reconstruction Technique (SIRT) iterative methods [*Ugalde et al.*, 2006].

3. Analysis and Results

[11] Because each analyzed frequency band is giving us information about inhomogeneous structures with sizes comparable to the seismic wavelengths, and given that the signal energy contents of the available data decays abruptly for frequencies f above 12 Hz, we decided to calculate the coda wave energy residuals [*Nishigami*, 1991; *Ugalde et al.*, 2006] for the frequency bands 4–8 (6 ± 2) Hz and 8–12 (10 ± 2) Hz, thus allowing us to image structures of sizes comparable to wavelengths of ~400 to ~800 m for 4–8 Hz, and ~300 m to ~400 m for 8–12 Hz. These sizes are derived by considering an average S-wave velocity of β = 3.3 km/s in the study region. From the bandpass-filtered seismograms, we calculated the rms amplitudes $A_{obs}(f|r, t)$ for each hypocentral distance r by using a 0.25 s spaced moving time window of length $t \pm 1$ s, and $t \pm 0.5$ s for the 6 Hz and 10 Hz center frequencies, respectively. The time interval for the analysis started at 1.5 times the S-wave travel times (in order to increase the resolution near the source region) and had a maximum length of 20 s (to minimize the effects of multiple scattering). We also computed the rms amplitudes for a noise window of 10 s before the P-wave arrival and only the amplitudes greater than two times the signal to noise ratio were kept. Then, the average decay curve was estimated for each seismogram by means of a linear regression of $\ln[t^2 A_{obs}(f|r, t)]$ vs. t, where the term t^2 is a geometrical spreading correction which is valid for body waves in a uniform medium. We only kept the estimates with a correlation coefficient (of the linear regression) greater than 0.60. The observed coda energy residuals $e(t)$ were then calculated by taking the ratio of the corrected observed amplitudes to the estimated exponential decay curve. Finally the residuals were averaged in time windows of δt = 0.25 s to get e_j at discrete lapse times t_j. The decrease of δt increases the spatial resolution, but also the size of the inversion problem.

[12] A 20 km × 20 km in horizontal and 50 km in depth study region was selected taking into account the distribution of stations and hypocenters. The study region was divided into $N = 50 \times 50 \times 50$ blocks, the volume of which satisfies the condition $\delta t \leq 2(\delta V)^{1/3}/\beta$. Then, the observational system of equations (1) was created by assuming the layered velocity structure shown in Table 1 and it was solved using the FBP algorithm [*Ugalde et al.*, 2006].

[13] To check for sampling insufficiencies, we computed the hit counts, or number of coda residuals contributed by each block. We found that the entire region is sampled by

Table 1. Layered Velocity Structure Model Considered[a]

Depth (km)	S-Wave Velocity (km/s)
4	2.0
2	2.1
0	2.2
−4	3.4
−22	3.8
−40	4.5

[a]D. Gómez (Vulcanological and Seismological Pasto Observatory, personal communication, 2005).

the ellipses although the number of hit counts is smaller at the deepest levels and also inside a shallow area to the north-east of the volcano summit.

[14] The resulting distribution of relative scattering coefficients $\alpha - 1$ in the study region for the analyzed frequency bands and for different depths up to 10 km from the summit is plotted in Figure 2. The colour scale indicates the perturbation of scattering coefficients from the average in this region, being the largest values ~3.0 and the minimum ~0.5. The stability of the solution was checked by decreasing δt and increasing the number of blocks. The resulting image showed the same distribution of strong and low scattering areas with slightly different values of the relative scattering coefficients.

4. Discussion and Conclusions

[15] Figure 2 shows that the region of ±10 km in horizontal and 10 km in depth centred at the Galeras volcano summit presents a remarkable inhomogeneous distribution of relative scattering coefficients. More than the 83% and 50% of the analyzed region for low and high frequencies, respectively, reveal a spatial perturbation of the scattering coefficient greater than +50%. For low frequencies, a strong scattering donut-shaped area with relative scattering coefficients between 0.96 and 3.0 is found around the volcano at all depths. The volume showing the strongest relative scattering coefficients ($\alpha - 1 \sim 2.0$–3.0) is located to the northeast of the volcano at depths between −0.5 km and −4.5 Km. At high frequencies, the strong scattering zone occurs slightly to the north of the axis of the volcano at the same depths. Also we may notice that the scattering strength is similar but slightly lower for the lower frequency band. Then, we may conclude that, at shallow depths, there is a single complex structure located at the north of the volcano that shows a frequency dependent behaviour. The relative scattering coefficients at high frequencies are stronger than those at low frequencies in a volume near the axis of the volcano, which means that the area contains small-size heterogeneities such as small fractures (comparable to a wavelength of ~300 m to ~400 m for a centre frequency of 10 Hz) which contribute more scattered energy than those with larger sizes. On the contrary, heterogeneities with sizes comparable to a wavelength of ~400 to ~800 m for a centre frequency of 6 Hz contribute more to the scattering energy at the north-east of the summit.

[16] Figure 3 shows a vertical cross section of the region along the east-west and north-south directions centred at the

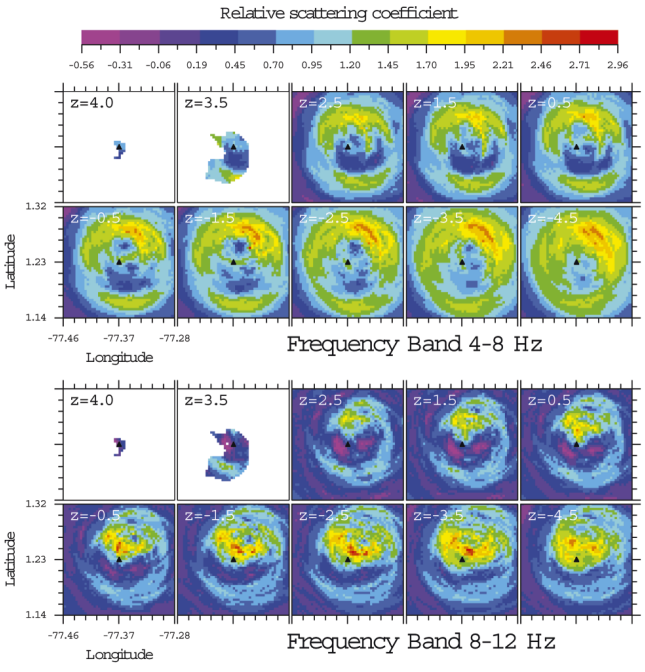

Figure 2. Horizontal sections of the study area showing the distribution of the relative scattering strength (α-1) at different depths from 4 km to −4.5 km. The solid triangle indicates the location of the Galeras volcano summit. The topographic contour lines at 4000 m and 3500 m levels are also plotted.

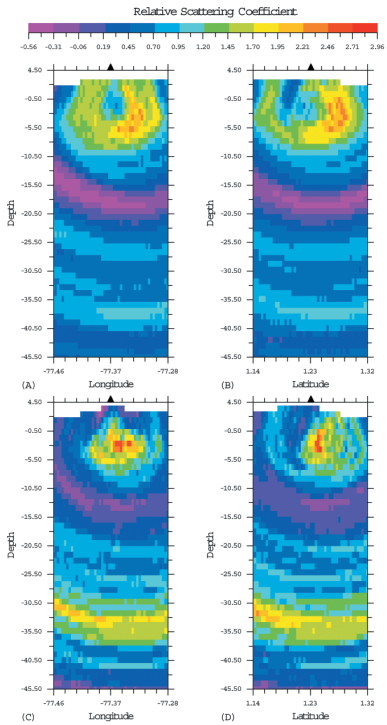

Figure 3. Vertical cross section of the study region along the two planes defined by the summit coordinates, which is indicated by the solid triangle (latitude 1.23° and longitude −77.36°). The color scale indicates the perturbation of the scattering coefficient α-1 for the (a and b) 4–8 Hz and (c and d) 8–12 Hz frequency bands.

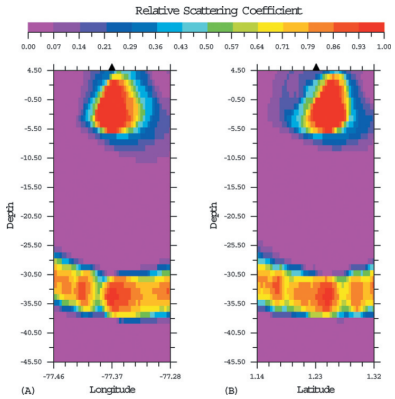

Figure 4. Vertical cross section showing the results of the inversion analysis for a synthetic test consisting of two spherical structures buried at depths of −2 km and −33 km.

volcano which shows the scattering perturbation at higher depths. A second strong scattering volume at depths between −29 km and −36 km is clearly observed at high frequencies and can be noticed at low frequencies. Unfortunately, in this case it is more difficult to establish the geometry of the scattering region. The ellipsoidal pattern imaged results from both a poor sampling and the geometry of the ellipses at these deeper levels, which are almost parallel. This makes it possible to establish only the depth and height of the region. A frequency dependence of the strength of the scattering coefficient is again observed thus indicating that small-scale heterogeneities contribute more scattering energy at these deeper levels.

[17] The existence of both structures is in close agreement with the current magmatic plumbing system model beneath Galeras volcano. This model is based on petrologic and seismic data and it proposes a shallow conduit system with a distinct reservoir at a depth of 4–5 km from the summit which is periodically fed from a deeper magma reservoir which is located from km's to tens of km's depth [*Calvache*, 1990; *Zapata et al.*, 1997]. In order to establish the validity of the results of this study and to help their geological interpretation, we tested the inversion method by means of a synthetic test. We simulated the presence of two magmatic chambers located at the north of the volcano at depths of −2 km and −33 km by two spherical structures with positive perturbations of the scattering coefficient embedded in a non perturbed medium. Thus, we assigned $\alpha_i - 1 = 1$ to the blocks located inside the spherical structures and $\alpha_i - 1 = 0$ to the blocks located outside. Then, we computed the corresponding coda energy residuals from the observational equation (1) using the same distribution of stations and events used in the analysis. Figure 4 shows the inversion of the synthesized residuals. It can be observed that both the pattern and the perturbation value of the scattering coefficient were well resolved in the considered region for shallow depths. A comparison of Figures 3 and 4 suggests a reasonable agreement between synthetic and experimental results, thus supporting the identification of the scattering structures imaged with the magmatic chambers of the geological model.

[18] **Acknowledgments.** We are very grateful to Diego Gómez and the people of the *Observatorio Vulcanológico y Sismológico de Pasto*, Colombia, for providing us with information about the recent activity history of the volcano and the seismic data used in this study.

References

Asano, Y., and A. Hasegawa (2004), Imaging the fault zones of the 2000 western Tottori earthquake by a new inversion method to estimate three-dimensional distribution of the scattering coefficient, *J. Geophys. Res.*, *109*, B06306, doi:10.1029/2003JB002761.

Banks, N. G., M. L. Calvache, and S. N. Williams (1997), ^{14}C ages and activity for the past 50 ka at Volcán Galeras, Colombia, *J. Volcanol. Geotherm. Res.*, *77*, 39–55.

Calvache, M. L. (1990), Geology and volcanology of the recent evolution of Galeras volcano, Colombia, M.S. thesis, 171 pp., La. State Univ., Baton Rouge.

Calvache, M. L., G. P. Cortés, and S. N. Williams (1997), Stratigraphy and chronology of the Galeras volcanic complex, Colombia, *J. Volcanol. Geotherm. Res.*, *77*, 5–19.

Chen, X., and L. T. Long (2000), Spatial distribution of relative scattering coefficients determined from microearthquake coda, *Bull. Seismol. Soc. Am.*, *90*, 512–524.

Gómez, D. M., and R. A. Torres (1997), Unusual low-frequency volcanic seismic events with slowly decaying coda waves observed at Galeras and other volcanoes, *J. Volcanol. Geotherm. Res.*, *77*, 173–193.

Kak, A. C., and M. Slaney (1988), *Principles of Computerized Tomographic Imaging*, IEEE Press, New York.

Nishigami, K. (1991), A new inversion method of coda waveforms to determine spatial distribution of coda scatterers in the crust and uppermost mantle, *Geophys. Res. Lett.*, *18*, 2225–2228.

Nishigami, K. (1997), Spatial distribution of coda scatterers in the crust around two active volcanoes and one active fault system in central Japan: Inversion analysis of coda envelope, *Phys. Earth Planet. Inter.*, *104*, 75–89.

Nishigami, K. (2000), Deep crustal heterogeneity along and around the San Andreas fault system in central California and its relation to segmentation, *J. Geophys. Res.*, *105*, 7983–7998.

Sato, H. (1977), Energy propagation including scattering effects; single isotropic scattering, *J. Phys. Earth*, *25*, 27–41.

Ugalde, A., E. Carcolé, and J. N. Tripathi (2006), Spatial distribution of scatterers in the crust by inversion analysis of coda envelopes: A case study of Gauribidanur seismic array (southern India), *Geophys. J. Int.*, in press.

Williams, S. N., M. L. Calvache, N. C. Sturchio, J. A. Zapata, R. A. Méndez, B. Calvache, A. Londoño, F. Gil, and Y. Sano (1990), Premonitory geochemical evidence of magmatic reactivation of Galeras volcano, Colombia, *Eos Trans. AGU*, *71*(17), 647.

Zapata, J. A., et al. (1997), SO_2 fluxes from Galeras volcano, Colombia, 1989–1995: Progressive degassing and conduit obstruction of a Decade volcano, *J. Volcanol. Geotherm. Res.*, *77*, 195–208.

E. Carcolé and A. Ugalde, Observatori de l' Ebre, CSIC—Universitat Ramon Llull, E-43520 Roquetes, Spain. (augalde@obsebre.es)

C. A. Vargas, Departamento de Geociencias, Universidad Nacional de Colombia, Ciudad Universitaria, Bogotá D.C., Colombia.